Achieving High Transmission and Q Bragg Filter via Balancing Dissipation and Radiation Loss

Yanliang Zhao, Jun Cao, Dejun Liu, Xi Shi, and Feng Liu

***Abstract*—Simultaneously high quality-factor (*Q*) and transmission (*T*) are highly desired in various optical, photonic, and optoelectronic applications such as filters, sensors, photodetectors and lasers. However, a trade-off between high *Q* and high *T* exists widely in optical systems thanks to the different physics triggers underneath. Here, as an example, we experimentally demonstrate a Bragg filter composed of niobium pentoxide (Nb_2O_5) and silica (SiO_2) stacks which enable high *Q* of 183 and high *T* of 91.3%. Balancing dissipation and radiation rate of the optical system is crucial to the performance of the device, which is validated by modulating the absorption of material (Nb_2O_5) and the number of stacks. Further, with the principle the tunable Bragg filter is able to work in a similar way at optical wavelengths, i.e., maintaining almost unchanged FWHM (full width at half-maximum) and *T* values. We believe our work offers an efficient strategy for achieving high *Q* and *T* optical systems to meet diversified application requests.**

***Index Terms*—High *Q* and *T*, trade-off, dissipation and radiation loss, niobium pentoxide, Bragg filter.**

I. Introduction

IN OPTICAL systems, high Q and high T have attracted great research interests since it is highly desired for applications in narrow-band filters, optical switches, lasers, sensors or even quantum information processing [1]–[5]. In general, high Q is achieved by exploiting Fabry-Pérot interferences, whispering gallery modes (WGM), defect modes, Fano resonances, and recent bounded states in the continuum (BICs) [6]–[11]. High T is obtained by matching the impedance at interfaces and using low-lossy material synergistically [12], [13]. However, a trade-off occurs commonly between Q and T since Q is determined by the sum of damping and radiation of the system, while T is dependent on the quotient of that two factors. This imposes great limitation on the exploration of optical applications with simultaneously high Q and high T. For examples, a typical quality factor of 10^2–10^3 was experimentally achieved in nanocavities, while, at the expenses of the T decreasing to the range between 0.2 and 0.7 [14].

Manuscript received June 29, 2021; revised July 29, 2021; accepted August 10, 2021. Date of publication August 18, 2021; date of current version September 14, 2021. This work was supported in part by the National Nature Science Foundation of China under Grants 12073018, 11704254, and U1931205, in part by Science and Technology Commission of Shanghai Municipality under Grants YDZX20203100002498, 19590746000, and 20070502400, and in part by Innovation Program of Shanghai Municipal Education Commission under Grant 2019-01-07-00-02-E00032. *(Corresponding authors: Xi Shi; Feng Liu.)*

The authors are with the Department of Physics, Key Laboratory for Submillimeter Astrophysics, Shanghai Normal University, Shanghai 200234, China (e-mail: 790050395@qq.com; caojun.081012@163.com; dejunliu1990@shnu.edu.cn; xishi@shnu.edu.cn; fliu@shnu.edu.cn).

Digital Object Identifier 10.1109/JPHOT.2021.3105116

Dielectric Bragg reflectors (DBRs) are one of the most popular photonic structures due to its clear physics and easy fabrications [15]. The DBRs usually act as flexible mirrors in the Fabry Pérot cavity, reducing the radiation loss and achieving high Q [16]. Moreover, most DBRs are composed of non-lossy layers or materials with very small extinction coefficients, e.g., ZnS, MgF_2 and Ta_2O_5 at optical wavelengths, in order to avoid the dissipation effect on cavity Q factor [17], [18]. Numerous optical systems based on DBR have been widely applied for color filters, lasers, photodetectors, bio-sensors and thermal radiators [19]–[21].

In this paper, we use the configuration of DBRs composing Nb_2O_5 and SiO_2 as an example to study the requirements of an optical system with simultaneously high Q and high T. We find the trade-off between radiation and dissipation rates of the system is crucial to the high optical performances, which are validated by coupled mode theory theoretically and the individual modulation of the radiation and dissipation rate experimentally. In our study, the radiation rate and the dissipation rate of the resonator are controlled via the number of Bragg stacks and the variable absorption of Nb_2O_5 films. With the revealed principle, we successfully fabricate a Bragg filter with high Q of 183 and high T of 91.3% in the visible frequencies. Intriguing, the transmission wavelength of the filter is tunable throughout the visible range with almost unchanged bandwidth and transmittance. We believe our results can boost tremendous interests in various applications which demands on high Q and high T such as Raman/fluorescence spectroscopy, photodetector, anti-counterfeiting and color filtering.

II. Theory Analyses and Simulations

We consider a resonant mode with a resonance frequency ω_0, corresponding dissipation loss rate γ_D, and radiation loss rate γ_R. The coupled mode equation for the resonant mode amplitude a with two ports can be written as [22]:

$$\frac{da}{dt} = (j\omega_0 - \gamma_D - \gamma_R)a + \begin{pmatrix} d_1 & d_2 \end{pmatrix} \begin{pmatrix} S_{1+} \\ S_{2+} \end{pmatrix}, \quad (1)$$

$$\begin{pmatrix} S_{1-} \\ S_{2-} \end{pmatrix} = e^{j\varphi} \begin{pmatrix} r & jt \\ jt & r \end{pmatrix} \begin{pmatrix} S_{1+} \\ S_{2+} \end{pmatrix} + \begin{pmatrix} d_1 \\ d_2 \end{pmatrix} a, \quad (2)$$

where d_1 and d_2 are the coupling coefficients of two ports. The scattering matrix $e^{j\varphi}\begin{pmatrix} r & jt \\ jt & r \end{pmatrix}$ describes the direct coupling between incoming and outcoming waves. The r and t are the

reflection and transmission coefficients, respectively. S_{1+} and S_{2+} are the amplitude of incoming wave from port 1 and port 2, while S_{1-} and S_{2-} are that for outgoing waves from two ports. To clarify the physical mechanism of Q and T, we start with a symmetrical structure and light is incident from port 1 for simplicity. As a result, assuming S_{2+} is 0, the T and Q are deduced as:

$$T = \frac{1}{(1+\frac{\gamma_D}{\gamma_R})^2}, \tag{3}$$

$$Q = \frac{1}{\omega_0\left(\gamma_R+\gamma_D\right)}. \tag{4}$$

The above equations clearly indicate that the T of the resonator is determined by γ_D/γ_R and the Q is inversely proportional to the total loss $\gamma_R+\gamma_D$. Smaller γ_D/γ_R and $\gamma_R+\gamma_D$ give rise to higher T and Q. Further inspection reveals that: (1) When the γ_D is fixed, higher Q requires smaller radiation loss which, on the contrary, decreases the transmission; A notable example of the case is the WGM micro-resonator which realize an ultra high Q (10^8) while low transmission (20%) [23]; (2) When the γ_R remains unchanged, smaller material dissipation leads to simultaneously high Q and T. For the dissipation loss, it usually depends on the intrinsic property of materials and hard to be actively modified. Thus, many articles focus on the modification of radiation losses via changing the structures of photonic resonators including grating, Fabry Pérot cavity, and metal-DBR structures. In these cases, the Q and T are manipulated but limited by varying the radiation loss only (e.g., grating, Fabry Pérot cavity, and metal-DBR structures can only reach the T of 70%, 55%, and 48% and the Q of 19, 14 and 54 respectively) [21], [24]–[26]. This limitation hampers the application implementations such as liquid crystal display [26]. The trade-off occurs inevitably even with different photonic structures from the physics viewpoint.

To validate the theoretical conclusions discussed above, we numerically investigate the Q and T of a dielectric Bragg filter with different number of stacks (N). The proposed structure is $(\mathrm{HL})^N(\mathrm{LH})^N$, as shown in Fig. 1(a). The H stands for the high-refractive-index Nb_2O_5 film which is widely used in optical devices and the L represents the low-refractive-index films (SiO_2) [27]–[29]. The optical thickness of each layer is $\lambda_0/4$ (133 nm). The refractive index of Nb_2O_5 is interpolated from experimental data (see Fig. 2(b)). Note that the extinction coefficient of Nb_2O_5 can be modulated according to the experimental results. In our simulation, the value of extinction coefficient is selected to be 0.001, which is one order of magnitude higher than the reported lowest absorption of Nb_2O_5 [30]. The refractive index of SiO_2 is 1.43 and the extinction coefficient is zero in the visible range. The calculated resonance frequency ω_0 is 564 THz ($\lambda_0 = 532$ nm) which agrees with the experimental results. Both the dissipation and radiation losses of the filter can be extracted from the calculated transmission spectrum by the transfer matrix method [31]. As the number of stacks increase from 2 to 10, the radiation loss of the filter drops rapidly from 36.00 to 0.04, and the dissipation loss varies slightly from 0.11

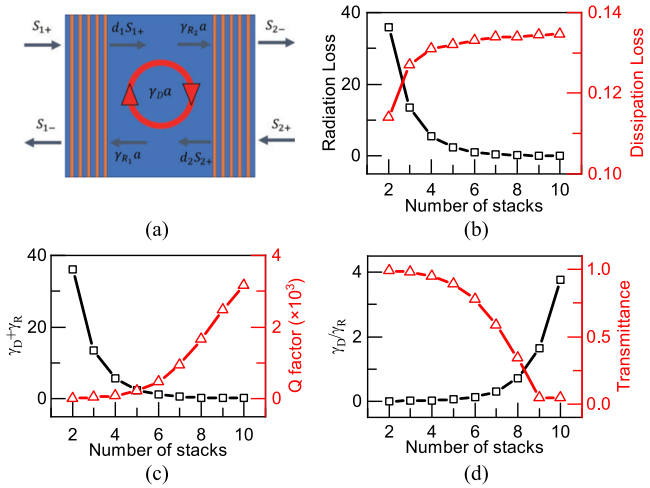

Fig. 1. (a) Schematic of the dielectric Bragg filter composed by Nb_2O_5 (orange) and SiO_2 (blue); (b) Dissipation loss (red triangle) and radiation loss (black square) for filters with different number of stacks (from 2 to 10); (c) Q (red triangle) and $\gamma_R+\gamma_D$ (black square) for filters with different number of stacks; (d) The maximum T (red triangle) and γ_D/γ_R (black square) for filters with different number of stacks. (Data in (b),(c), and (d) are retrieved from TMM-calculated spectra).

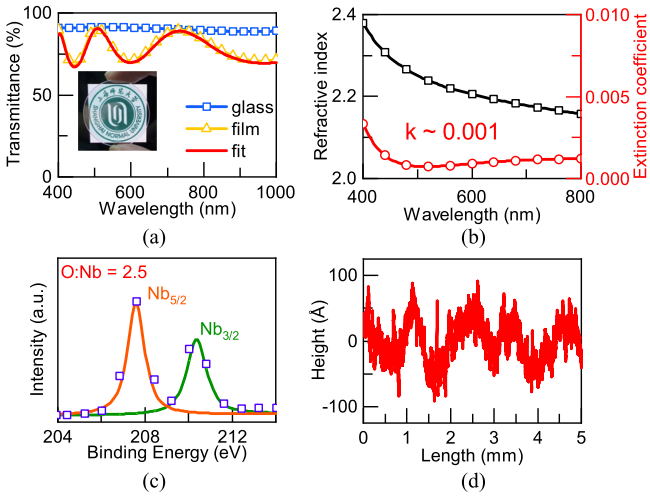

Fig. 2. (a) Transmission spectra of the glass substrate (blue square), 330 nm Nb_2O_5 films deposited on glass (yellow triangle), and the fitting result (red line) with normal incidence; (b) Extinction coefficient (red circle) and refractive index (black square) of Nb_2O_5 film; (c) X-ray photoelectron spectroscopy of Nb_2O_5 films; (d) The roughness of the film detected by stylus profiler.

to 0.13 (see Fig. 1(b)). These results show that the radiation loss of the filter is dominantly affected by the number of stacks and the dissipation loss is mainly determined by materials in this system. As expected, with the number of stacks increases, the Q increases from 14 to 3000 owning to the decreasing total losses ($\gamma_R+\gamma_D$) (see Fig. 1c), however, the T decreases from 1 to near 0 as the ratio of dissipation loss to radiation loss(γ_D/γ_R) increases from 0.003 to 3.800 (see Fig. 1(d)). As a result, the trade-off between high Q and high T requires the number of film stacks to be 5 or 6 in this system.

III. Experimental Results

The Bragg stacks composed by Nb_2O_5 and SiO_2 are deposited on the glass substrate by Ion-beam assisted electron beam coating system (Leybold Ares-1110) with the chamber pressure less than 8.0×10^{-6} mBar. The evaporation rate is set to 0.2 nm/s for Nb_2O_5 and 0.5 nm/s for SiO_2. During the evaporation of Nb_2O_5, different oxygen fluxes of 0, 10 and 30 sccm are injected into a 4-kW ion source in order to modulate the extinction coefficient of films. The chamber's temperature is kept at 160 °C during deposition. Before evaporation, the glass substrates are ultra-sonicated in 99.9 % alcohol for 15 minutes, then rinsed with deionized water.

The transmittance of 330 nm thickness Nb_2O_5 films with 30 sccm oxygen flux is measured by the UV-visible spectrophotometer (MAPADA UV-3200) is shown in Fig. 2(a). The highest transmittance is 91.4%, close to the substrate (glass). The refractive index and extinction coefficients of the Nb_2O_5 films fitted by the envelope method are shown in Fig. 2(b) [32]. The refractive index of Nb_2O_5 films is 2.26 at 500 nm. The extinction coefficient of the film is about 0.001 in the visible range. Fig. 2(c) shows the X-ray photoelectron spectroscopy of Nb 3d from Nb_2O_5 films. The spectrum reveals $3d_{\frac{5}{2}}$ and $3d_{\frac{3}{2}}$ peaks at about 207 and 210 eV, according to Nb^{5+}. These results illustrate that the prepared film is Nb_2O_5 without any incomplete oxide [33]. In addition, the Nb_2O_5 film's roughness is less than 3 nm in a large area (5 mm × 5 mm). The above properties indicate that Nb_2O_5 has great potential in the fabrication of dielectric Bragg filters with high Q and high T.

With the Bragg filters composed of well-controlled Nb_2O_5 and SiO_2 films, we experimentally investigate the effects of γ_R and γ_D on the Q and T. Firstly, we study the influence of radiation loss rate by varying the number of stacks of the Bragg filters. With the given extinction coefficient of Nb_2O_5 0.001, the Q and T of the Bragg filters with 2, 5 and 8 stacks are shown in Fig. 3(a) and 3(c), respectively. The T decreases from 92%, 41% to 5%, and the Q increases from 11, 114 to 297 as the number of stacks increase from 2, 5 to 8, respectively. These results clearly show the trade-off between Q and T induced by γ_R. Secondly, we study the influence of dissipation loss rate γ_D on Q and T by varying the extinction coefficient of Nb_2O_5. For the given stack number of 5, Fig. 3(b) and 3(d) show both the T and Q of the filter decrease as the extinction coefficient of Nb_2O_5 increases from 0.001 to 0.100. All the experimental results are in good agreement with the aforementioned theoretical discussion and results. To summarize, the strategy to obtain high Q and high T device is to use either material with smaller dissipation or balance the radiation and dissipation of the system if the material dissipation is fixed.

IV. Applications

Understanding the above strategy, we fabricate a dielectric Bragg filter with both high Q and high T by choosing the number of stacks 5 and the Nb_2O_5 with the extinction coefficient of 0.001. A SiO_2 defect layer is inserted into the DBR structure, which induces a narrow passing band [6], [34], [35]. As shown

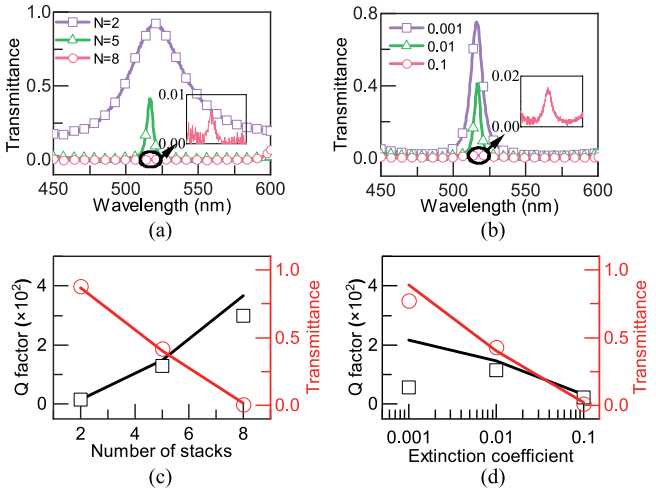

Fig. 3. (a) The transmission spectra of filters with different number of stacks (N = 2, 5, 8); (b) The transmission spectra of filters composed of Nb_2O_5 films with different extinction coefficients (k ≈ 0.001, 0.01 and 0.1); (c),(d) The comparison between simulations and experiments of Q (black square) and the T (red cycle) (the lines are the numerical results and the dots are the experiment results).

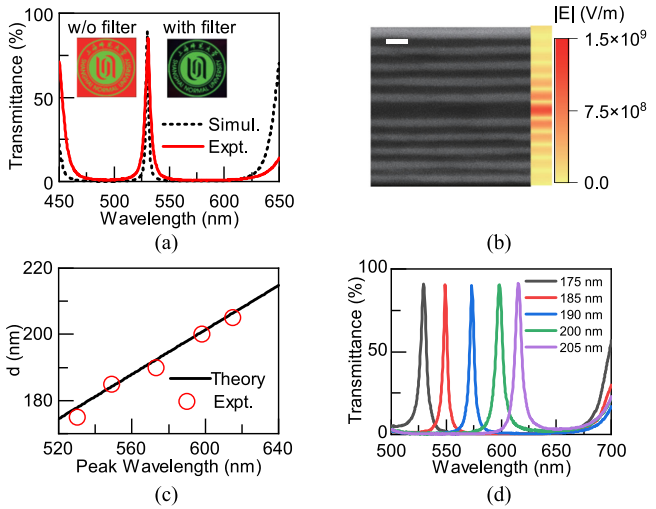

Fig. 4. (a) Comparison between experimental (red line) and simulation (black dashed line) results for the dielectric Bragg filter; (b) Cross-section view and corresponding field distribution (the scale bar is 100 nm); (c) Comparison between experimental (red circle) and theoretical (black line) results; (d) Experimental transmission spectra corresponding to the thicknesses of different defect layers.

in Fig. 4(a), the measured transmittance of the filter shows overall consistence with the simulation results. The vibration in 450 nm and 650 nm regions between simulation and experiment is mainly caused by the inconsistency of the actual film thickness with the simulated film thickness (The mean error amounts to 5%). Our devices successfully achieve high Q (183) and high T (91.3%) simultaneously, comparable to other works and even commercial products (see Table I) [36], [37]. Compared with the fabricated filters enabled by other optical systems, the overall performances of the fabricated Bragg filter are also impressive (see Table II) [38]–[42]. The insets of Fig. 4(a) illustrate the excellent color filtering performance. Furthermore, we note here that the Q and T of the fabricated Bragg filter can be improved

TABLE I
PERFORMANCES OF THE OPTICAL FILTERS BASED ON DBR

Bragg structure	CWL (nm)	FWHM (nm)	Q factor	T (%)	Ref/Company
Bragg filter (Nb_2O_5 and SiO_2)	549	3	183	91.3	this work
Bragg filter with chirped layers (Nb_2O_5 and SiO_2)	650	7	93	58	[36]
Bragg filter (Ta_2O_5 and SiO_2)	1115	40	28	97	[37]
Commercial Bragg filter	532/514	5/2.3	106.4/223	85/90	TECHSPEC/ALLUXA
Metal(Pt)-DBR (Ge/SiO_2)	4500	5.7	780	A=80%	[21]
Fabry-Pérot Cavity (Ag/ZnS/Ag)	540	38	14	55	[25]
Metal(Ag)-DBR(Ta_2O_5/SiO_2)	536	10	53.6	48	[19]

* The CWL stands for center wavelength. A and R represent for absorption and reflection of structure.

TABLE II
PERFORMANCES OF THE OPTICAL FILTERS BASED ON DIFFERENT OPTICAL MODES

Optical mode	CWL (nm)	FWHM (nm)	Q factor	T (%)	Ref
Defect mode (Bragg filter)	549	3	183	91.3	this work
Defect mode (2D photonic crystal)	550	70	7.8	R=70%	[38]
Whispering gallery mode	1550	1.55×10^{-5}	1×10^{8}	20	[23]
Magnetic resonance mode	1550	200	7.8	A=97%	[24]
Fano mode	930	8	116	A=99%	[39]
Guided mode	850	1.3	634	A=80%	[40]
Plasmon-induced transparency mode	780	8	97	60	[41]
BIC mode	0.7 THz	0.016 THz	44	90	[42]

* The CWL stands for center wavelength. A and R represent for absorption and reflection of structure, respectively.

to higher or more impressive level by using the Nb_2O_5 with smaller extinction coefficient (e.g., $1e^{-4}$ reported in Ref [30]). The SEM image of the stacking structure of the DBR and the corresponding electric field distribution are shown in the Fig. 4(b).

Furthermore, the optical filters with different thickness of defect layers are also simulated and fabricated. It can be observed that the filters corresponding to the defect layer with different thicknesses have different transmission wavelengths. Benefiting from the high ratio of two materials' refractive indices, transmission peaks can be adjusted in a wide range in the forbidden band. As the thickness of defect layer increases from 175 to 185, 190, 200, and 205 nm, the pass band position shifts from 530 (Q: 106) to 549 (183), 573 (143), 598 (100), and 615 nm (95), which coincides with formula $\lambda = 2nd$, where λ is the transmission wavelength, n is the refractive index of defect layer, and d is the thickness of defect layer (see Fig. 4(c), (d)). Also, the average T exceeds 90%. In contrast to other kinds of filters, the FWHM and T of our structures are almost unchanged with resonance frequencies because of the relatively fixed radiation loss and dissipation loss of structures [19], [25]. Thanks to the features of the structure and the material, we can independently adjust the dissipation loss and radiation loss rate of the resonator precisely to achieve required Q and T of applications by changing the coating process parameters and the number of stacks. We believe that the fabricated Bragg filter has the potentiality to be used in Raman/fluorescence spectroscopy, photodetector, color filtering and anti-counterfeiting [20], [43].

V. CONCLUSION

In summary, we theoretically and experimentally investigate the physical mechanism of Q and T of dielectric Bragg filter. The Q is inversely proportional to total loss, and the T is determined by the ratio of radiation loss to dissipation loss. The Bragg filters composed by Nb_2O_5 and SiO_2 with different Q and T are obtained by adjusting the radiation loss (number of stacks) and dissipation loss (absorption of films). The narrow-band optical filter with a high Q (189) and high T (91.3%) is fabricated with an optimal design. It's notable that the transmission peak of the filter can be adjusted in the visible range without changing the FWHM and T. Besides, by synergistically adjusting the radiation loss and the dissipation loss of the structure, we can design filters with different Q and T to meet diverse application requirements. Our works pave the way to design high performance of photonic resonators.

Disclosures: The authors declare no conflicts of interest.

REFERENCES

[1] T. Tanemura, Y. Takushima, and K. Kikuchi, "Narrowband optical filter, with a variable transmission spectrum, using stimulated brillouin scattering in optical fiber," *Opt. Lett.*, vol. 27, no. 17, pp. 1552–1554, Sep. 2002.
[2] N. Moll, R. Harbers, R. F. Mahrt, and G. L. Bona, "Integrated all-optical switch in a cross-waveguide geometry," *Appl. Phys. Lett.*, vol. 88, no. 17, Apr. 2006, Art. no. 171104.
[3] L. He, A. K. Ozdemir, and L. Yang, "Whispering gallery microcavity lasers, WGM microlasers," *Laser Photon. Rev.*, vol. 7, no. 1, pp. 60–82, Jan. 2013.

[4] T. Maier, G. Strasser, and E. Gornik, "Monolithic integration of vertical-cavity laser diodes and resonant photodetectors with hybrid Si_3N_4 & SiO_2 top Bragg mirrors," *IEEE Photon. Technol. Lett.*, vol. 12, no. 2, pp. 119–121, Feb. 2000.

[5] M. H. Devoret and R. J. Schoelkopf, "Superconducting circuits for quantum information: An outlook," *Science*, vol. 339, no. 6124, pp. 1169–1174, Mar. 2013.

[6] C.-J. Wu and Z.-H. Wang, "Properties of defect modes in one-dimensional photonic crystals," *PIER*, vol. 103, pp. 169–184, 2010.

[7] V. S. Ilchenko, A. A. Savchenkov, A. B. Matsko, and L. Maleki, "Nonlinear optics and crystalline whispering gallery mode cavities," *Phys. Rev. Lett.*, vol. 92, Jan. 2004, Art. no. 043903.

[8] B.-S. Song, S. Noda, T. Asano, and Y. Akahane, "Ultra-high q. photonic double-heterostructure nanocavity," *Nature Mater.*, vol. 4, no. 3, pp. 207–210, 2005.

[9] F. Liu, L. Chen, Q. Guo, J. Chen, X. Zhao, and W. Shi, "Enhanced graphene absorption and linewidth sharpening enabled by fano-like geometric resonance at near-infrared wavelengths," *Opt. Exp.*, vol. 23, no. 16, pp. 21097–21106, 2015.

[10] B. Wang *et al.*, "High q plasmonic resonances: Fundamentals and applications," *Adv Opt. Mater.*, vol. 9, Apr. 2021, Art. no. 2001520.

[11] K. Koshelev, S. Lepeshov, M. Liu, A. Bogdanov, and Y. Kivshar, "Asymmetric metasurfaces with high- resonances governed by bound states in the continuum," *Phys. Rev. Lett.*, vol. 121, no. 19, Nov. 2018, Art. no. 193903.

[12] Y.-L. Liu *et al.*, "Controllable optical response by modifying the gain and loss of a mechanical resonator and cavity mode in an optomechanical system," *Phys. Rev. A*, vol. 95, 2017, Art. no. 013843.

[13] N. Liu *et al.*, "Plasmonic analogue of electromagnetically induced transparency at the drude damping limit," *Nature Mater.*, vol. 8, no. 9, pp. 758–762, Sep. 2009.

[14] Y.-C. Lin, S.-H. Chou, and W.-J. Hsueh, "Robust high-Q filter with complete transmission by conjugated topological photonic crystals," *Sci. Rep.*, vol. 10, Dec. 2020, Art. no. 7040.

[15] C. K. Madsen and J. H. Zhao, in *Optical Filter Design and Analysis: A Signal Processing Approach*. Hoboken, NJ, USA: Wiley, 1999.

[16] P. Qiu, B. Wu, P. Fu, M. Li, Y. Xie, and Q. Kan, "Fabrication and characterization of low-threshold single fundamental mode VCSELs with dielectric DBR mirror," *IEEE Photon J.*, vol. 13, no. 4, 2021, Art. no. 1500106.

[17] G. Kedawat *et al.*, "Fabrication of artificially stacked ultrathin ZnS/MgF multilayer dielectric optical filters," *ACS Appl. Mater. Interfaces*, vol. 5, no. 11, pp. 4872–4877, Jun. 2013.

[18] C.-J. Tang, C.-C. Jaing, K.-S. Lee, and C.-C. Lee, "Residual stress in Ta_2O_5-SiO_2 composite thin-film rugate filters prepared by radio frequency ion-beam sputtering," *Appl. Opt.*, vol. 47, no. 13, pp. C167-C171, May. 2008.

[19] C.-C. Chang, T.-Y. Chen, T.-W. Lin, J. Leng, K. Tamada, and Y.-J. Lee, "Flexible and ultranarrow transmissive color filters by simultaneous excitations of triple resonant eigenmodes in hybrid metallic-optical tamm state devices," *ACS Photon.*, vol. 8, no. 2, pp. 540–549, Feb. 2021.

[20] M. Furchi *et al.*, "Microcavity-integrated graphene photodetector," *Nano Lett.*, vol. 12, no. 6, pp. 2773–2777, Jun. 2012.

[21] Z. Wang, J. K. Clark, Y.-L. Ho, S. Volz, H. Daiguji, and J.-J. Delaunay, "Ultranarrow and wavelength-tunable thermal emission in a hybrid metal-optical tamm state structure," *ACS Photon.*, vol. 7, no. 6, pp. 1569–1576, Jun. 2020.

[22] K. X. Wang, "Time-reversal symmetry in temporal coupled-mode theory and nonreciprocal device applications," *Opt. Lett.*, vol. 43, no. 22, pp. 5623–5626, Nov. 2018.

[23] D. K. Armani, T. J. Kippenberg, S. M. Spillane, and K. J. Vahala, "Ultra-high-Q toroid microcavity on a chip," *Nature*, vol. 424, no. 6926, pp. 925–928, 2003.

[24] J. B. Lassiter *et al.*, "Third-harmonic generation enhancement by film-coupled plasmonic stripe resonators," *ACS Photon.*, vol. 1, no. 11, pp. 1212–1217, Nov. 2014.

[25] K.-T. Lee, S. Y. Han, Z. Li, H. W. Baac, and H. J. Park, "Flexible high-color-purity structural color filters based on a higher-order optical resonance suppression," *Sci. Rep.*, vol. 9, 2019, Art. no. 14917.

[26] J. H. Park *et al.*, "High transmittance and deep RGB primary electrochromic color filter for high light out-coupling electro-optical devices," *Opt. Exp.*, vol. 27, no. 18, , pp. 25531–25543, Sep. 2019.

[27] R. A. Rani, A. S. Zoolfakar, A. P. O"Mullane, M. W. Austin, and K. Kalantar-Zadeh, "Thin films and nanostructures of niobium pentoxide: Fundamental properties, synthesis methods and applications," *J. Mater. Chem. A*, vol. 2, no. 38, pp. 15683–15692, Jul. 2014.

[28] Aagard and L. R., "Optical waveguide characteristics of reactive dc-sputtered niobium pentoxide films," *Appl. Phys. Lett.*, vol. 27, no. 11, pp. 605–607, Dec. 1975.

[29] C. C. Lee, C. L. Tien, and J. C. Hsu, "Internal stress and optical properties of Nb_2O_5 thin films deposited by ion-beam sputtering," *Appl. Opt.*, vol. 41, no. 10, pp. 2043–2047, Apr. 2002.

[30] F. Lai, L. Lin, Z. Huang, R. Gai, and Y. Qu, "Effect of thickness on the structure, morphology and optical properties of sputter deposited Nb_2O_5 films," *Appl. Surf. Sci.*, vol. 253, no. 4, pp. 1801–1805, Dec. 2006.

[31] C. Qu *et al.*, "Tailor the functionalities of metasurfaces based on a complete phase diagram," *Phys. Rev. Lett.*, vol. 115, no. 23, Dec. 2015, Art. no. 235503.

[32] J. C. Manifacier, J. Gasiot, and J. P. Fillard, "A simple method for the determination of the optical constants n, k and the thickness of a weakly absorbing thin film," *J. Phys. E: Sci. Instrum.*, vol. 9, no. 11, pp. 1002–1004, Nov. 1976.

[33] C. Xu, Y. Zhao, Y. Qiang, Y. Zhu, L. Guo, and J. Shao, "Comparison of laser-induced damage in Ta_2O_5 and Nb_2O_5 single-layer films and high reflectors," *Chin. Opt. Lett.*, vol. 9, no. 1, Jan. 2011, Art. no. 013102.

[34] E. Yablonovitch, "Inhibited Spontaneous Emission in Solid-State Physics and Electronics," *Phys. Rev. Lett.*, vol. 58, no. 20, pp. 2059–2062, May 1987.

[35] S. John, "Strong localization of photons in certain disordered dielectric superlattices," *Phys. Rev. Lett.*, vol. 58, no. 23, pp. 2486–2489, 1987.

[36] M. Taimoor, S. Reuter, H. Hillmer, and T. Kusserow, "Narrowband optical thin-film filters with distributed cavity modes," *Appl. Phys. A*, vol. 122, May 2016, Art. no. 538.

[37] L. Chen, H. Nishimura, K. Fukumi, J. Nishii, and K. Hirao, "Fabrication of multilayer thin film filters by hydrofluoric acid bonding," *Appl. Surf. Sci.*, vol. 253, no. 11, pp. 4906–4910, Mar. 2007.

[38] E.-H. Cho *et al.*, "Two-dimensional photonic crystal color filter development," *Opt. Exp.*, vol. 17, no. 10, pp. 8621–8629, May 2009.

[39] M. Zhang, J. Fang, F. Zhang, J. Chen, and H. Yu, "Ultra-narrow band perfect absorbers based on fano resonance in MIM metamaterials," *Opt. Commun.*, vol. 405, pp. 216–221, Dec. 2017.

[40] D. Chanda *et al.*, "Coupling of plasmonic and optical cavity modes in quasi-three-dimensional plasmonic crystals," *Nat. Commun.*, vol. 2, Sep. 2011, Art. no. 479.

[41] J. Wang *et al.*, "A novel planar metamaterial design for electromagnetically induced transparency and slow light," *Opt. Exp.*, vol. 21, no. 21, pp. 25159–25166, Oct. 2013.

[42] D. Liu, X. Yu, F. Wu, S. Xiao, F. Itoigawa, and S. Ono, "Terahertz high-q quasi-bound states in the continuum in laser-fabricated metallic double-slit arrays," *Opt. Exp.*, vol. 29, no. 16, pp. 24 779–24 791, 2021.

[43] M. Kolle *et al.*, "Mimicking the colourful wing scale structure of the papilio blumei butterfly," *Nature Nanotech*, vol. 5, no. 7, pp. 511–515, Jul. 2010.